Langmuir
Article
pubs.acs.org/Langmuir
© 2009 American Chemical Society

Effects of Ligand Coordination Number and Surface Curvature on the Stability of Gold Nanoparticles in Aqueous Solutions

Bing C. Mei,[†,‡] Eunkeu Oh,[†] Kimihiro Susumu,[†] Dorothy Farrell,[†] T. J. Mountziaris,[‡] and Hedi Mattoussi*[,†]

[†]*Division of Optical Sciences, Naval Research Laboratory, Washington, D.C. 20375, and* [‡]*Department of Chemical Engineering, University of Massachusetts, Amherst, Massachusetts 01003*

Received April 22, 2009. Revised Manuscript Received May 23, 2009

The colloidal stability of gold nanoparticles (AuNPs) cap-exchanged with either monothiol- or dithiolane-terminated PEG-OCH_3 ligands was investigated. Three distinct aspects were explored: (1) effects of excess salt concentration; (2) ligation competition by dithiothreitol (DTT); and (3) resistance to sodium cyanide digestion. We found that overall ligands presenting higher coordination numbers (dithiolane) exhibit much better stability to excess added salt and against competition from DTT compared to their monodentate counterparts. Resistance to NaCN digestion indicated that there is a balance between coordination number and density of ligand packing on the NP surface. For smaller NPs, where a larger surface curvature reduces the ligand packing density, a higher coordination number is clearly beneficial. In comparison, a higher ligand density allowed by the smaller curvature for larger nanocrystals makes monothiol−PEG-capped NPs more resistant to cyanide digestion. The present study indicates that balance between the coordination number and surface packing density is crucial to enhancing the colloidal stability of AuNPs.

Downloaded via FLORIDA STATE UNIV on January 5, 2024 at 02:13:00 (UTC).
See https://pubs.acs.org/sharingguidelines for options on how to legitimately share published articles.

Introduction and Background

Inorganic nanoparticles such as those made of metallic, semiconducting, and magnetic materials have attracted tremendous interest for use in biological and medical applications.[1−4] In particular, there has been extensive work aimed at developing gold nanoparticles (AuNPs) as scattering and/or plasmonic probes, as platforms for drug delivery, and for localized heat treatment of cancer tissue.[5−7] These applications require that the nanoparticle be stable in buffer solutions and in biological media, which are rich in salt and thiol compounds (e.g., glutathione, cysteine). Water-soluble AuNPs that are uniform in size, stable over a broad pH range and in the presence of high ion concentrations, and surface-functionalized with target reactive groups/functions are thus desired for most of these applications.

A common approach for promoting hydrophilicity and bioconjugation of AuNPs has involved the use of cap exchange or surface modification of citrate-capped nanoparticles often with thiol-terminated ligands.[8,9] These include thiol-terminated poly(ethylene glycol)s (PEGs), DNAs, and aptamers. This strategy promotes interparticle steric hindrance, prevents nanoparticle aggregation in buffer solutions, and permits control over their interface with the surrounding solution/environment; citrate-functionalized AuNPs are charge-stabilized and tend to aggregate in the presence of added salts.[9,10] Because citrate reduction and stabilization provide AuNPs with a size regime spanning ∼2 to 100 nm, an array of nanoparticles with different sizes and capped with a variety of functional ligands can be made using this simple ligand-exchange strategy.[11,12] As a result, tremendous effort has been invested in developing surface ligands that enhance the stability and biocompatibility of AuNPs.

We should also emphasize that there has been an effort geared toward the synthesis of AuNPs (also known as monolayer-protected clusters, MPC) via a two-phase reaction starting with alkanethiol ligands.[13] If a hydrophilic segment is appended onto the ligands, water-soluble nanoparticles can be made using this route.[14] Whereas these nanoparticles are a substantial improvement compared to their water-insoluble predecessors, these methods are limited with respect to the accessible range of nanoparticle sizes.

Ligand-to-nanocrystal binding (such as thiol-to-AuNPs) is usually driven by metal chelation (or coordination) of the anchoring group onto the surface, not by covalent coupling, which makes this interaction rather weak. This implies that ligands presenting multiple chelating groups should produce stronger affinity/anchoring to the metallic surface. We have indeed shown that dithiol-terminated ligands provide substantially enhanced stability to CdSe-ZnS core−shell quantum dots (as compared to single thiol ligands) in aqueous solutions.[15−17]

*Corresponding author. E-mail: hedi.mattoussi@nrl.navy.mil.

(1) Rosi, N. L.; Mirkin, C. A. *Chem. Rev.* **2005**, *105*, 1547–1562.
(2) *Nanobiotechnology II: More Concepts and Applications*; Mirkin, C. A., Niemeyer, C. M., Eds.; Wiley-VCH: Darmstadt, Germany, 2007.
(3) Sperling, R. A.; Rivera Gil, P.; Zhang, F.; Zanella, M.; Parak, W. J. *Chem. Soc. Rev.* **2008**, *37*, 1896–908.
(4) De, M.; Ghosh, P. S.; Rotello, V. M. *Adv. Mater.* **2008**, *20*, 1–17.
(5) Wijaya, A.; Hamad-Schifferli, K. *Langmuir* **2008**, *24*, 9966–9969.
(6) Hamad-Schifferli, K.; Schwartz, J. J.; Santos, A. T.; Zhang, S. G.; Jacobson, J. M. *Nature* **2002**, *415*, 152–155.
(7) Jain, P. K.; Huang, X.; El-Sayed, I. H.; El-Sayad, M. A. *Plasmonics* **2007**, *2*, 107–118.
(8) Daniel, M. C.; Astruc, D. *Chem. Rev.* **2004**, *104*, 293–346.
(9) Love, J. C.; Estroff, L. A.; Kriebel, J. K.; Nuzzo, R. G.; Whitesides, G. M. *Chem. Rev.* **2005**, *105*, 1103–1169.
(10) Mei, B. C.; Susumu, K.; Medintz, I. L.; Delehanty, J. B.; Mountziaris, T. J.; Mattoussi, H. *J. Mater. Chem.* **2008**, *18*, 4949–4958.
(11) Frens, G. *Nat. Phys. Sci.* **1973**, *241*, 20–22.
(12) Zhang, S. S.; Leem, G.; Srisombat, L. O.; Lee, T. R. *J. Am. Chem. Soc.* **2008**, *130*, 113–120.
(13) Brust, M.; Walker, M.; Bethell, D.; Schiffrin, D. J.; Whyman, R. *J. Chem. Soc., Chem. Commun.* **1994**, 801–802.
(14) Wuelfing, W. P.; Gross, S. M.; Miles, D. T.; Murray, R. W. *J. Am. Chem. Soc.* **1998**, *120*, 12696–12697.
(15) Mattoussi, H.; Mauro, J. M.; Goldman, E. R.; Anderson, G. P.; Sundar, V. C.; Mikulec, F. V.; Bawendi, M. G. *J. Am. Chem. Soc.* **2000**, *122*, 12142–12150.
(16) Uyeda, H. T.; Medintz, I. L.; Jaiswal, J. K.; Simon, S. M.; Mattoussi, H. *J. Am. Chem. Soc.* **2005**, *127*, 3870–3878.
(17) Susumu, K.; Uyeda, H. T.; Medintz, I. L.; Pons, T.; Delehanty, J. B.; Mattoussi, H. *J. Am. Chem. Soc.* **2007**, *129*, 13987–13996.

One would expect that the colloidal stability of surface-modified AuNPs should also benefit from using ligands that present multiple chelating groups, as was demonstrated for quantum dots. The advantages offered by multidentate ligands for binding to AuNPs compared to their single-point-coordination counterparts have been an open question because monothiol-terminated ligands and receptors have performed relatively well in functional assays.[14,18] There are a few reports demonstrating the advantages of functionalizing AuNPs with oligonucleotides and alkanes appended with multiple thiols,[19−23] but we are unaware of anyone comparing the stability of AuNPs capped with monothiol versus multithiol-appended PEG ligands. PEGylated ligands promote affinity to water and reduce nonspecific interactions in biological media. In addition, if end-functionalized PEG ligands are used, the resulting NPs can be coupled to a variety of target receptors while providing control over the number of receptors per NP (conjugate valence); low valences can also be achieved with this strategy.

In this study, we investigated the stability of AuNPs under a variety of conditions following cap exchange with modular PEG ligands presenting either mono- or dithiol anchoring groups. In particular, we probed their stability in the presence of excess salts against competition from dithiothreitol (DTT) as well as their resistance to sodium cyanide (NaCN)-induced digestion. One main characteristic that distinguishes the present study from other stability studies reported in the literature is that our system features a more extensive modification of the nanoparticle surface, where a nearly complete removal of the native ligands and their replacement with new ones is realized. In comparison, literature reports involve controllable numbers of thiol-terminated oligonucleotide ligands self-assembled onto the nanoparticle surface, in addition to the native citrate cap, resulting in small numbers of thiol-terminated oligonucleotides per NP.[19,20] Moreover, our 1,2-dithiolane-terminated ligands feature two closely spaced sulfur groups (constrained by the five-membered ring structure), which may provide better coordination to the NP surface compared to thiol-terminated oligonucleotides, where thiols are appended at the end of rather long chains.[19]

Results and Discussion

To probe the effects of the coordination number on the colloidal stability of surface-modified AuNPs, we synthesized two modular PEG-based ligands; one is appended with a single thiol, and the other presents a disulfide group (Figure 1 inset). The remaining modules of the ligands, namely, the short alkyl chain and the methoxy-terminated PEG segment, are identical for both sets. The bidentate ligand consists of a thioctic acid covalently appended onto a methoxy-terminated PEG (mPEG, MW $\approx$ 750 Da) through an amide bond. It was prepared via a simple three-step reaction as reported in ref 10. First, the hydroxy terminal group of commercially available mPEG was transformed to a methanesulfonyl group with methanesulfonyl chloride and then to an azide using sodium azide. Next, the terminal azide group was

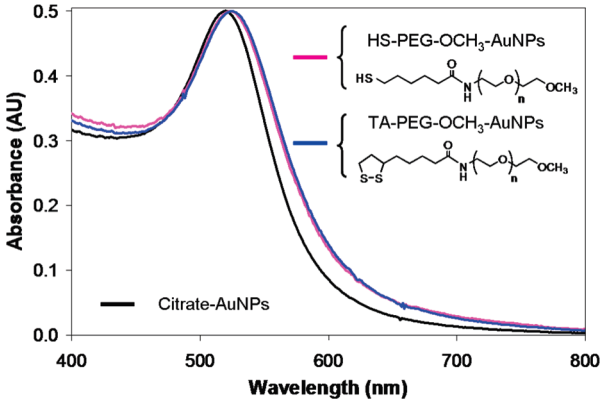

Figure 1. Absorption spectra of 15 nm AuNP dispersions in DI H_2O: as-purchased citrate-stabilized (black), cap-exchanged with HS-PEG750-OCH_3 (purple), and cap-exchanged with TA-PEG750-OCH_3 (blue).

reduced to an amine using triphenylphosphine, yielding amino-mPEG (H_2N-PEG-OCH_3). Finally, thioctic acid (TA) was attached to the amine terminal group via *N*,*N*′-dicyclohexylcarbodiimide (DCC) coupling to form TA-PEG-OCH_3. The monodentate ligand was synthesized using the same H_2N-PEG-OCH_3 precursor in two steps: (1) 6-(acetylthio)-hexanoic acid was coupled to H_2N-PEG-OCH_3 via DCC to form acetyl-protected thiol-mPEG (AcS-PEG-OCH_3), followed by (2) cleavage of the acetyl group using sodium methoxide to obtain the final HS-PEG-OCH_3 ligand (Figure 1 inset).[24,25] Further details on the synthesis of the monothiol ligands can be found in the Supporting Information. Citrate-stabilized AuNPs with different sizes (5, 10, and 15 nm) used in this study were purchased as colloidal gold solutions from Ted Pella, Inc. (Reading, CA). When performing cap exchange with HS-PEG-OCH_3 and TA-PEG-OCH_3 ligands, the number of excess ligands used was adjusted, depending on the AuNP concentration of the citrate-stabilized stock solutions and the size of the nanoparticles used, to maintain a constant ratio of ligand-to-Au surface atoms (larger AuNPs contain more surface atoms per particle). We also adjusted the excess molar concentration of ligands used for HS-PEG-OCH_3 to twice that of TA-PEG-OCH_3 in order to account for the difference in the coordination number of the two ligands (i.e., the total number of thiol groups added to a given concentration of AuNP solution and the size of AuNPs is equivalent for both ligands). We used ligand molar concentrations ~800 and ~400 times that of the concentration of Au surface atoms for mono- and dithiol ligands, respectively. (Further details can be found in the Supporting Information.) Because of the rather large excess ligands used for cap exchange, we anticipate that the resulting NPs will have their surfaces saturated with the PEGylated ligands. We confirmed the effectiveness of the cap exchange by comparing the FT-IR spectra collected from dispersions of TA-PEG-OCH_3-capped and HS-PEG-OCH_3-capped AuNPs and free ligands. A representative example is shown for TA-PEG-AuNPs (Supporting Information). Data showed that bands attributed to the amide C=O stretch (at 1670 cm^{-1}) and amide N−H bending (at 1540 cm^{-1}), measured for free ligands, were maintained in the spectra measured for TA-PEG-OCH_3-AuNP dispersions.[10] Gel electrophoresis experiments were less conclusive because irreversible aggregation of the citrate-stabilized AuNPs occurred immediately after loading in

(18) Storhoff, J. J.; Elghanian, R.; Mucic, R. C.; Mirkin, C. A.; Letsinger, R. L. *J. Am. Chem. Soc.* **1998**, *120*, 1959–1964.
(19) Li, Z.; Jin, R. C.; Mirkin, C. A.; Letsinger, R. L. *Nucleic Acids Res.* **2002**, *30*, 1558–1562.
(20) Dougan, J. A.; Karlsson, C.; Ewen Smith, W.; Graham, D. *Nucleic Acids Res.* **2007**, *35*, 3668–3675.
(21) Srisombat, L. O.; Park, J. S.; Zhang, S.; Lee, T. R. *Langmuir* **2008**, *24*, 7750–7754.
(22) Hill, H. D.; Millstone, J. E.; Banholzer, M. J.; Mirkin, C. A. *ACS Nano* **2009**, *3*, 418–424.
(23) Cederquist, K. B.; Keating, C. D. *ACS Nano* **2009**, *3*, 256–260.
(24) Pengo, P.; Broxterman, Q. B.; Kaptein, B.; Pasquato, L.; Scrimin, P. *Langmuir* **2003**, *19*, 2521–2524.
(25) Svedhem, S.; Hollander, C. A.; Shi, J.; Konradsson, P.; Liedberg, B.; Svensson, S. C. T. *J. Org. Chem.* **2001**, *66*, 4494–4503.

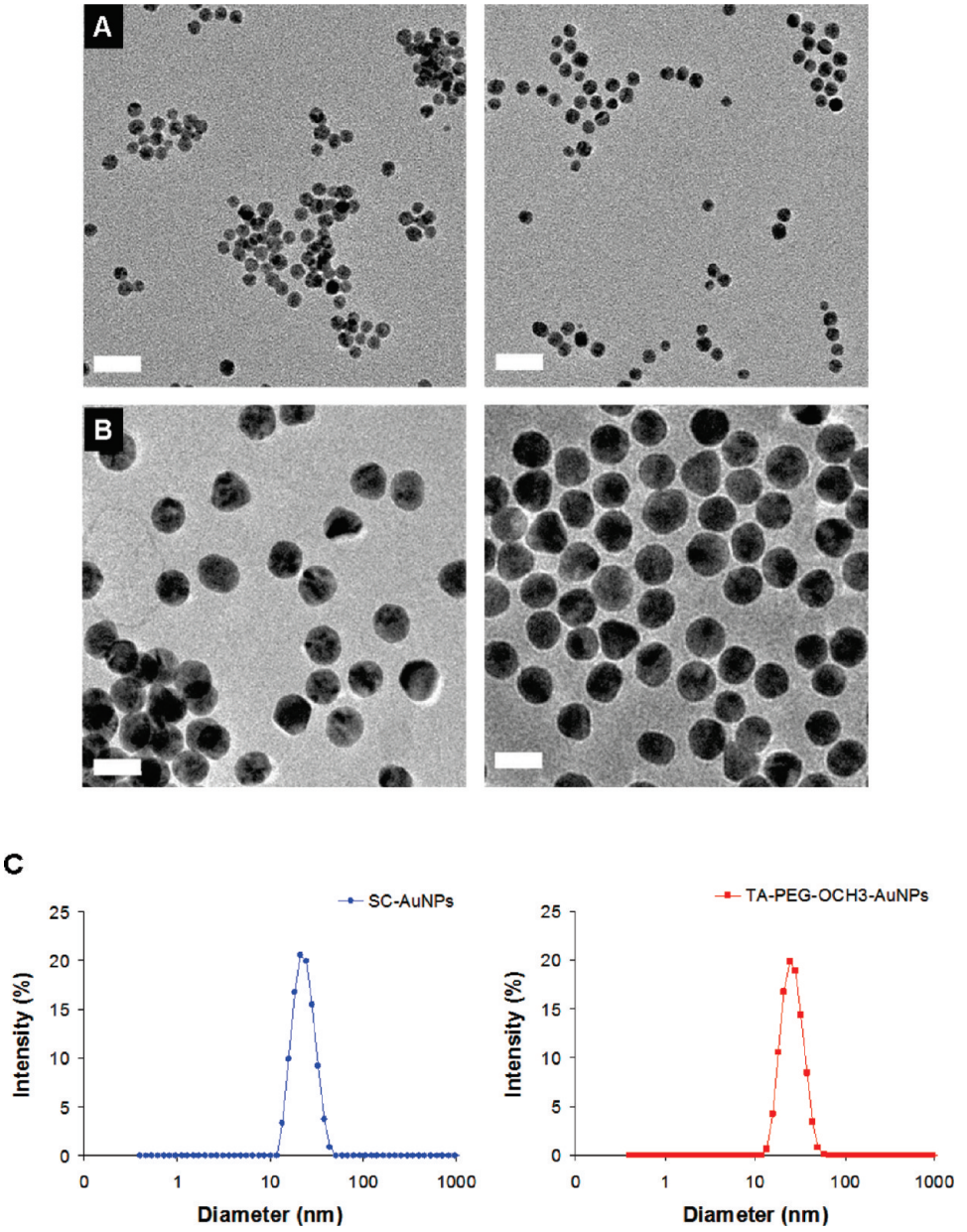

Figure 2. TEM images and DLS data of AuNPs before and after cap exchange with TA-PEG-OCH_3. (A) Five nanometer NPs citrate-stabilized AuNPs (left) and after cap-exchange (right). The measured diameter was 6.1 ± 0.6 nm (for citrate-stabilized) and 5.8 ± 0.6 nm (for TA-PEG-capped). (B) Fifteen nanometer AuNPs before (left) and after cap exchange (right). The measured diameter was 15.9 ± 0.9 nm (for citrate-stabilized) and 16 ± 1 nm (for TA-PEG-capped). The white bars shown in all panels indicate a 20 nm scale. (C) Intensity versus size distribution curves extracted from the autocorrelation function provided by DLS experiments collected from the 15 nm NP dispersions; the average hydrodynamic diameter ($2R_H$) extracted from DLS was ~23.5 nm for sodium citrate-stabilized (SC) and ~26.5 nm for TA-PEG-OCH_3-capped nanocrystals, respectively. Both measurements indicate no reduction in the NP size after cap exchange.

the gel well (caused by the presence of excess ions and EDTA in the loading buffer);[26] TA-PEG-OCH_3-AuNPs did not aggregate in the loading buffer but showed a negligible shift, indicative of an overall neutral NP surfaces. These measurements indicate that nearly complete replacement of the native citrate ligands by the new thiol-appended ligands has been achieved. A very small number of the native ligands may persist, nonetheless, given the nature of the cap exchange process. The more intrusive replacement of the surface ligands realized with our nanocrystals contrasts with stability studies conducted using oligonucleotide-modified AuNPs; in those studies, a maximum of ~100−200 ligands per AuNP (13 nm size) was used.[18−20] Because 13 nm AuNPs present ca. 7300 surface atoms,[8] this implies that oligonucleotide-to-Au atom ratios ≪1 (~0.03 in this particular case) were used in those studies.

Figure 1 shows the absorption spectra for 15 nm AuNPs cap-exchanged with both sets of ligands along with that of the original citrate-stabilized dispersion. Data indicate that the main absorption characteristics of the nanoparticles, namely, the surface plasmon peak location and shape, before (as purchased) and after cap exchange with the new ligands are preserved; a slight red shift of the plasmon peak (~1−3 nm) is sometimes measured for the newly capped NPs, compared to their citrate-stabilized AuNP precursors. Similar behavior was recorded for nanoparticles with different sizes. The ability of both ligands to effectively displace

(26) Olmedo, I.; Araya, E.; Sanz, F.; Medina, E.; Arbiol, J.; Toledo, P.; Alvarez-Lueje, A.; Giralt, E.; Kogan, M. J. *Bioconjugate Chem.* **2008**, *19*, 1154–1163.

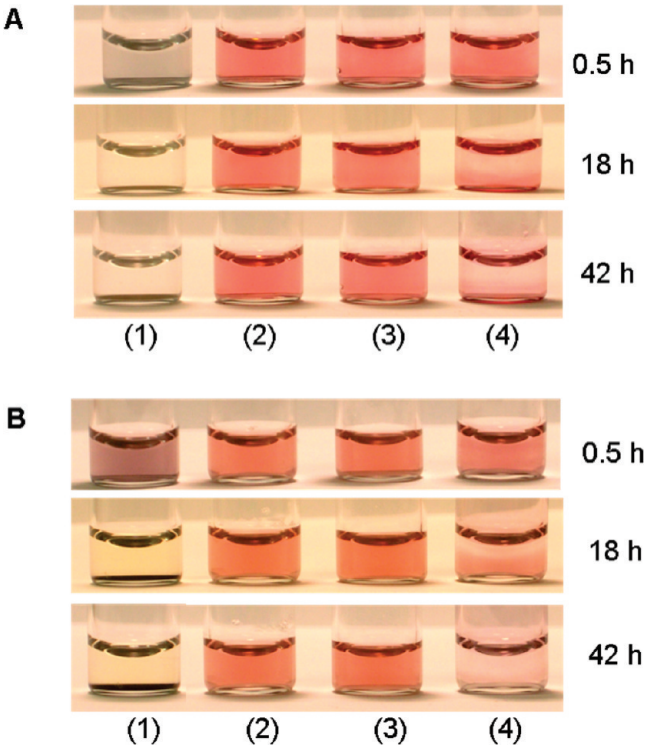

Figure 3. Stability of AuNP dispersions under various conditions: 15 nm (A) and 5 nm (B). (Column 1) Sodium citrate-stabilized AuNPs in 1 M NaCl and (column 2) TA-PEG-OCH_3-AuNPs in DI H_2O, which serve as positive (aggregated) and negative (aggregation-free) control samples, respectively. (Column 3) TA-PEG-OCH_3-AuNPs and (column 4) HS-PEG-OCH_3-AuNPs; both have 1 M NaCl added.

the native citrate on the AuNP surface results from the strong affinity of the terminal thiol groups (soft base) to the gold surface (soft acid).[8,27,28]

To test if the thiol ligands have any deleterious effects on the AuNP integrity (due, for example, to potential etching of surface atoms, etc., an issue discussed in ref 29 for Au clusters), the nanoparticles were examined using transmission electron microscopy (TEM) and dynamic light scattering (DLS) before and after cap exchange. Additional experimental details and data analysis on TEM and DLS are provided in the Supporting Information. TEM images were collected from 5 and 15 nm NPs, and DLS was applied only to dispersions of the 15 nm NPs; weak scattering prevented the collection of reliable DLS data for the 5 nm AuNPs. The TEM images shown in Figure 2A,B indicate that there is no change in particle size or distribution following cap exchange for both sets of nanocrystals. TEM data also showed that during transfer onto the carbon grid, citrate-stabilized NPs often exhibited signs of aggregation and clumping. In comparison, TA-PEG-OCH_3-AuNPs always provided well-dispersed distributions of NPs on the grid regardless of size. Figure 2C shows the intensity versus size distribution curves extracted from the autocorrelation function provided by DLS. Plots in Figure 2C show that monomodal NP distributions characterize both dispersions, with hydrodynamic sizes that are consistently larger than those extracted from TEM as expected.[30,31] DLS data also indicate that there is a slight increase in the hydrodynamic diameter measured for the TA-PEG-OCH_3-AuNPs compared to that for the citrate-stabilized NPs; such an increase arises from differences in the contributions of the hydrodynamic interactions to the measured diffusion coefficient for both sets of dispersions. The TA-PEG ligand has a larger lateral extension and results in a slightly larger contribution than from citrate functions.[31]

The first test probed the effects of excess salt on the colloidal stability of cap-exchanged AuNPs. Excess ions can influence the solubility of nanoparticles in two ways. If the steric stabilization of nanoparticles in solution is controlled by electrostatic repulsions, as is the case with citrate-stabilized AuNPs, added excess salt will reduce the Debye screening length, hence causing van der Waals attractions to become dominant and induce NP aggregation. Added excess counterions can also alter the solubility of the surface-bound ligands to the surrounding solvent, thus promoting aggregation buildup. We found that dispersions of citrate-stabilized AuNPs become unstable in the presence of added NaCl, with macroscopic aggregation occurring at salt concentrations as low as 100 mM (Figure 3, column 1 shows solutions containing 1 M NaCl). In comparison, both HS-PEG-OCH_3-AuNPs and TA-PEG-OCH_3-AuNPs exhibited better stability to added NaCl, which indicates that effective cap exchange has taken place (Figure 3). In addition, no change in the absorption features was measured for these dispersions after salt addition (Supporting Information); the AuNP solubility is now controlled by the hydrophilic nature of the PEG segment. Dispersions of 15 and 5 nm TA-PEG-OCH_3-AuNPs were stable in the presence of 1 M NaCl for at least 6 months. However, although initially stable in 1 M NaCl solutions, we found that for HS-PEG-OCH_3-AuNPs aggregation built up after 18 h of storage at room temperature (column 4 in Figure 3A,B); macroscopic aggregation of these NP dispersions was observed after 2 days of storage.

The second test probed the competition by small-molecule DTT for coordination onto the AuNP surface; this provided an additional means of assessing the binding strength of both PEG-appended ligands to the nanocrystals. DTT is a common reducing agent often used to break disulfide bonds of proteins and other thiol-containing biomolecules.[32,33] At high concentration, DTT can effectively displace the thiol ligands away from the NP surface, resulting in progressive particle aggregation; this competition ultimately depends on the affinity of the initial ligand to the Au surface.[20] DTT-induced NP aggregation can occur more rapidly in the presence of excess NaCl because of added screening effects. DTT competition and displacement of the ligands alter the spectroscopic properties of the sample and are manifested in a decrease in the SPB peak, along with an increase in the absorbance at longer wavelengths. The resistance of the capping ligand to the competing molecules was tested by collecting the absorption spectra of the cap-exchanged AuNPs in the presence of DTT and NaCl and by following the rates at which the SPB value decreased and/or the absorption spectrum red-shifted with time (Figure 4). We quantified this competition process by defining an aggregation factor (AF) as the ratio between the optical densities at 615 nm and at the SPB (~524 nm) because changes in solution absorbance due to aggregation were most noticeable at these two wavelengths in our experiments.[34] The change in the absorption tail around 610−650 nm is reflective of NP-to-NP association

(27) Pearson, R. G. *J. Chem. Educ.* **1968**, *45*, 581–588.
(28) Garcia, B.; Salome, M.; Lemelle, L.; Bridot, J. L.; Gillet, P.; Perriat, P.; Roux, S.; Tillement, O. *Chem. Commun.* **2005**, 369–371.
(29) Schaaff, T. G.; Whetten, R. L. *J. Phys. Chem. B* **1999**, *103*, 9394–9396.
(30) Mattoussi, H.; Cumming, A. W.; Murray, C. B.; Bawendi, M. G.; Ober, R. *Phys. Rev. B* **1998**, *58*, 7850–7863.
(31) Pons, T.; Uyeda, H. T.; Medintz, I. L.; Mattoussi, H. *J. Phys. Chem. B* **2006**, *110*, 20308–20316.
(32) Agasti, S. S.; You, C. C.; Arumugam, P.; Rotello, V. M. *J. Mater. Chem.* **2008**, *18*, 70–73.
(33) Kumar, A.; Whitesides, G. M. *Appl. Phys. Lett.* **1993**, *63*, 2002–2004.
(34) Amendola, V.; Meneghetti, M. *J. Mater. Chem.* **2007**, *17*, 4705–4710.

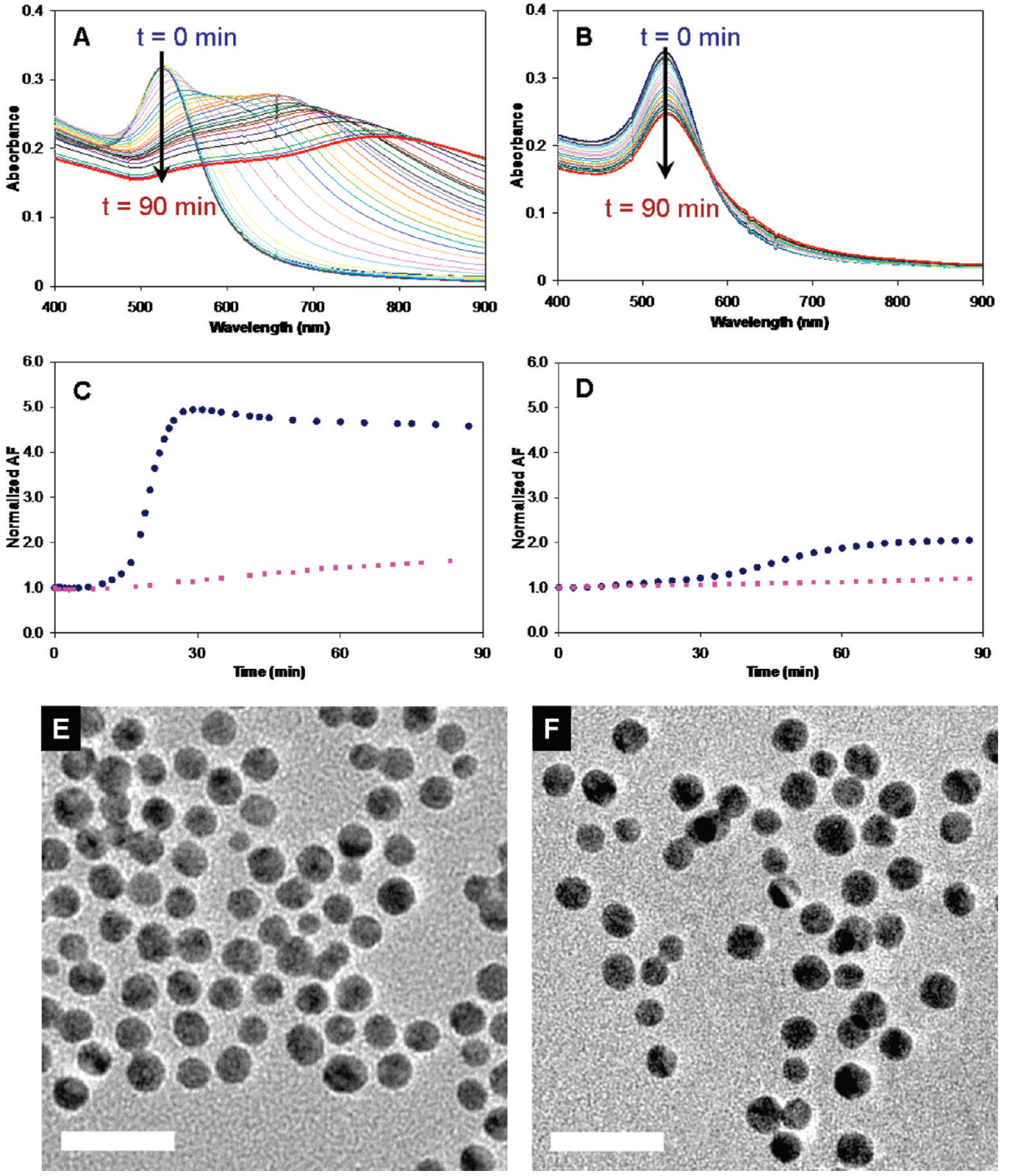

Figure 4. Stability test of HS-PEG-OCH_3-AuNPs and TA-PEG-OCH_3-AuNPs to DTT competition. All samples have 1 M DTT and 400 mM NaCl added. (A, B) Time course of the absorption spectra of 15 nm AuNPs capped with HS-PEG-OCH_3 and TA-PEG-OCH_3, respectively. (C, D) Normalized aggregation factor (AF) of 15 and 5 nm AuNPs, respectively, extracted from the data in plots A and B. TA-PEG-OCH_3-AuNPs (red squares) and HS-PEG-OCH_3-AuNPs (blue circles). Data consistently show that the TA-PEG-OCH_3-capping of AuNPs provides stronger resistance to DTT competition than HS-PEG-OCH_3 capping, independent of the AuNP size. TEM images of AuNPs (5.5 nm nominal size) following exposure to DTT for HS-PEG-OCH_3-capped NPs (E) and TA-PEG-OCH_3-capped NPs (F); images were collected 18 h after sample preparation. The white bars indicate a 20 nm scale.

(due to reduced steric stabilization), which builds up in the sample and ultimately results in aggregation. A progressive change in the solution color accompanies a loss in its colloidal stability. We should note that the exact location of the SPB can vary by ~1−3 nm, depending on the solution and NP size. Using this parameter also reduces (compensates for) effects of small fluctuations in the absorption spectra with time due to variations in the excitation intensity. If the water-soluble AuNPs are unstable in the presence of DTT and NaCl, then the aggregation factor will increase with time. Conversely, if the ligand's affinity to the Au surface is strong, then DTT competition becomes ineffective and the nanoparticles stay well dispersed even in the presence of salt. In this instance, the absorption spectra along with AF would remain either unaltered or exhibit a slow change with time. Figure 4A,B shows the time progress of the absorption spectra of 15 nm AuNPs cap-exchanged with either HS-PEG-OCH_3 or TA-PEG-

Table 1. Parameters Involved in NaCN Digestion[a]

NP size (nm)	ε	$N_{T\text{-}Au}$/NP	$N_{S\text{-}Au}$/NP	O.D. (0.5 cm)	[AuNP] (M)	[$N_{T\text{-}Au}$] (M)	[$N_{S\text{-}Au}$] (M)	[NaCN] (M)	CN/$N_{S\text{-}Au}$ ratio	CN/$N_{T\text{-}Au}$ ratio
5	9.70×10^6	3.85×10^3	1002	0.3	6.19×10^{-8}	2.38×10^{-4}	6.20×10^{-5}	7.00×10^{-3}	113	29
10	9.55×10^7	3.08×10^4	4412	0.3	6.28×10^{-9}	1.94×10^{-4}	2.77×10^{-5}	6.10×10^{-2}	2201	315
15	3.64×10^8	1.04×10^5	9612	0.3	1.65×10^{-9}	1.71×10^{-4}	1.58×10^{-5}	6.80×10^{-2}	4292	397

[a] The O.D. of the dispersions was ~0.6. ε is the NP extinction coefficient. [AuNP] is the AuNP concentration, $N_{T\text{-}Au}$, designates the total number of Au atoms per nanoparticle. $N_{S\text{-}Au}$ designates the number of surface Au atoms per nanoparticle. [$N_{T\text{-}Au}$] and [$N_{S\text{-}Au}$] are the corresponding molar concentrations.

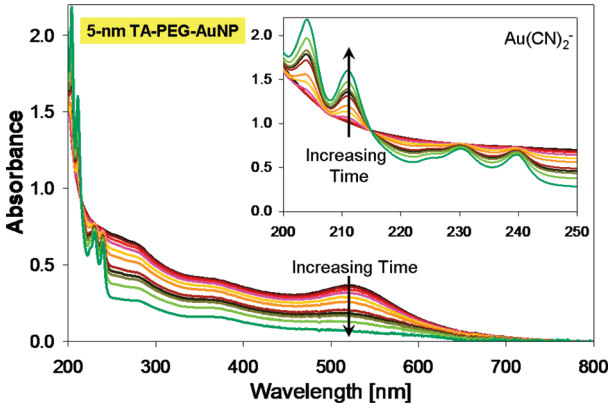

Figure 5. Representative progression of the absorption spectra collected in the presence of sodium cyanide: the surface plasmon band (SPB) decreases while the absorption peaks of $Au(CN)_2^-$ (expanded in the inset) increase with time; both features reflect a progressive digestion of the nanoparticles by added NaCN. The chemical reaction involved in the digestion is $4Au + 8NaCN + O_2 + 2H_2O \rightarrow 4NaAu(CN)_2 + 4NaOH$. The data shown are for 5 nm TA-PEG-OCH_3-AuNPs in 7 mM NaCN solution over the course of 3.5 h.

OCH_3 in the presence of 1 M DTT and 400 mM NaCl, respectively. Figure 4C shows the corresponding progression of AF with time. Solutions of TA-PEG-OCH_3-AuNPs exhibited no signs of aggregate buildup whereas that of HS-PEG-OCH_3-AuNPs showed macroscopic aggregation after 90 min. The data clearly show that AuNPs capped with bidentate TA-PEG-OCH_3 exhibited a much stronger resistance to aggregation (and thus better dispersion stability) than those capped with HS-PEG-OCH_3. Solutions of HS-PEG-OCH_3-AuNPs progressively changed color from red to violet to black with time as macroscopic aggregates progressively formed in the samples. Additional data on AF vs time for mono- and dithiol-appended ligands for 5 nm AuNPs are shown in Figure 4D. We should emphasize that the changes exhibited in the solution properties upon addition of DTT are primarily attributed to the loss/alteration of NP solubility. There are no measured changes in the NP morphology or size for NPs capped with either ligand (Figure 4E,F). These side-by-side comparisons of behaviors observed for mono- versus dithiol cap-exchanged nanoparticles suggest that the dominating factor in providing stable AuNPs against small-molecule competition is the number of coordinating groups, which defines the ligand binding strength to the metal surface. Enhanced stability in water was also reported for AuNPs prepared using thioctic acid-modified oligonucleotides as solubilizing/stabilizing ligands.[20] The oligonucleotides were attached to *N*-hydroxysuccinimidyl (NHS) ester-modified TA prior to cap exchange on citrate-stabilized AuNPs.

In the third test, we focused on the ligand's ability to "protect" the nanoparticles against sodium cyanide (NaCN) digestion. Although the strength of the interactions between ligands and surface atoms is significant, as shown in the DTT competition experiments above, this test probed additional effects such as density and packing of the capping monolayer, which can determine the ligand's ability to shield the inorganic core against strongly etching CN anions.[8,9,32] When CN anions come into contact with the inorganic core, they form complexes with the gold atoms, progressively etching the nanoparticle surface. This converts the reddish AuNPs sample into a colorless solution of $Au(CN)_2^-$ ions.[35–37] In our experiments, the concentration of NaCN added to the dispersions was increased for the large nanocrystals (i.e., 7 mM for 5 nm, 61 mM for 10 nm, and 68 mM for 15 nm nanocrystals). This was done to compensate for the increasing surface as well as total number of Au atoms per NP for larger nanocrystals. Table 1 shows the values for surface ($N_{S\text{-}Au}$) and total ($N_{T\text{-}Au}$) Au atom concentrations along with the corresponding CN/N_{S-Au} and CN/$N_{T\text{-}Au}$ ratios used; further details on how to derive those values from the experimental parameters are provided in the Supporting Information. The increase was not proportional, nonetheless, with the CN/$N_{T\text{-}Au}$ molar ratio varying from ~30 for 5 nm NPs to ~400 for 15 nm NPs. We selected NaCN concentrations that allow the digestion of all three sizes of nanoparticles on similar time scales (~2 to 3 h), where the ability of CN ions to access Au atoms inside the nanoparticle widely varies with increasing size; CN ions complex to the Au atoms (and remove them) layer by layer as they digest the nanoparticle. Importantly, this should not affect the comparison because for each size of NPs the same NaCN concentration was used for both ligands.

Figure 5 shows the progression of the absorption spectrum with time collected for the 5 nm AuNP solution following the addition of 7 mM NaCN. There is a clear decrease in the absorption spectrum with time for $\lambda > 250$ nm. Figure 5 also shows that new features appear in the spectrum for $\lambda < 250$ nm with well-defined peaks at 204, 211, 230, and 240 nm (signatures of $Au(CN)_2^-$ formation) that become increasingly visible with time (Figure 5 inset).[38,39] We quantified the rate of decomposition by measuring the time-dependent decrease of the SPB absorbance and fitting it to a first-order exponential decay function

$$y = y_0 \times \exp\left(-\frac{t}{t_D}\right) \quad (1)$$

where t_D is the decay time and y_0 is the absorbance value at $t=0$.[24,40] For these experiments, the initial absorbance of the NP solutions at the SPB was maintained at ~0.3 (in a 0.5 cm optical path cuvette), but the concentration of NaCN used was raised with

(35) Weisbecker, C. S.; Merritt, M. V.; Whitesides, G. M. *Langmuir* **1996**, *12*, 3763–3772.
(36) Canumalla, A. J.; Al-Zamil, N.; Phillips, M.; Isab, A. A.; Shaw, C. F. *J. Inorg Biochem.* **2001**, *85*, 67–76.
(37) Love, C. S.; Ashworth, I.; Brennan, C.; Chechik, V.; Smith, D. K. *J. Colloid Interface Sci.* **2006**, *302*, 178–186.
(38) Mie, G. *Ann. Phys.* **1908**, *25*, 377–445.
(39) Templeton, A. C.; Wuelfing, M. P.; Murray, R. W. *Acc. Chem. Res.* **2000**, *33*, 27–36.
(40) Isaacs, S. R.; Cutler, E. C.; Park, J. S.; Lee, T. R.; Shon, Y. S. *Langmuir* **2005**, *21*, 5689–5692.

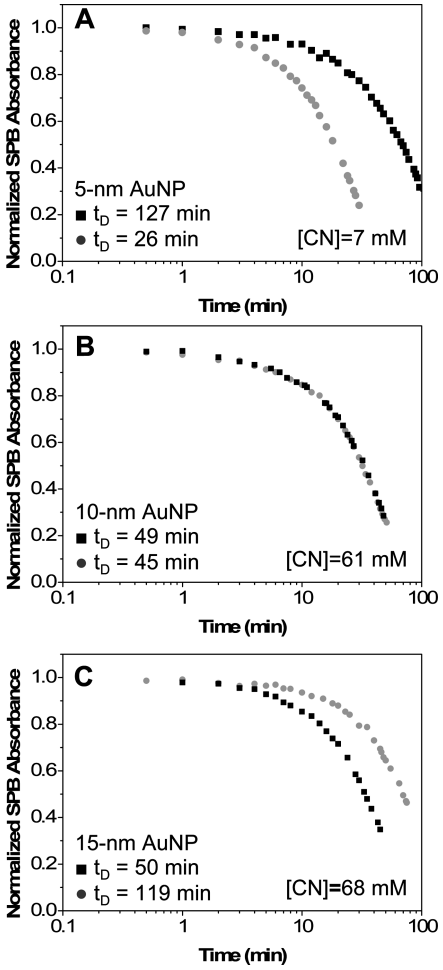

Figure 6. Cyanide digestion of TA-PEG-OCH_3-capped (black squares) and HS-PEG-OCH_3-capped (gray circles) AuNPs of various sizes: (A) 5, (B) 10, and (C) 15 nm. The concentration of NaCN used for each data set and their respective decay constants are also reported.

increasing AuNP size. (See Supporting Information for additional details.) A comparison of mono- versus dithiol capping indicates that NP digestion by added NaCN depends on the nanoparticle size (Figure 6). Data indicate that as the NP size increased from 5 to 15 nm the relative ability of the ligands to protect the inorganic core from cyanide digestion changed. Whereas TA-PEG-OCH_3-AuNPs exhibited a much slower digestion rate than their single-thiol analog for 5 nm nanoparticles (t_D was ~5 times longer for TA-PEG-OCH_3 ligands, Figure 6A), the trend was reversed for the larger 15 nm NPs (t_D was ~2.5 times longer for HS-PEG-OCH_3 ligands, Figure 6C). Similar decomposition curves were measured for the intermediate 10 nm NPs capped with either ligand (t_D was essentially the same for both set of caps, see Figure 6B).

This result is very informative; it indicates that NP resistance to NaCN digestion is affected by a combination of ligand footprint (related to the coordination number of the anchoring group) and packing density on the nanocrystal surface (as schematically sketched in Figure 7).[22,23] TA-PEG ligands have a larger footprint than their monothiol counterparts, and this implies that a given surface area can accommodate a higher number of HS-PEG-OCH_3 than TA-PEG-OCH_3 species. The lateral volume that a ligand tail can explore away from the surface is, however, dependent on the nanoparticle surface curvature. A small nanocrystal presents a higher surface curvature, which in turn provides a

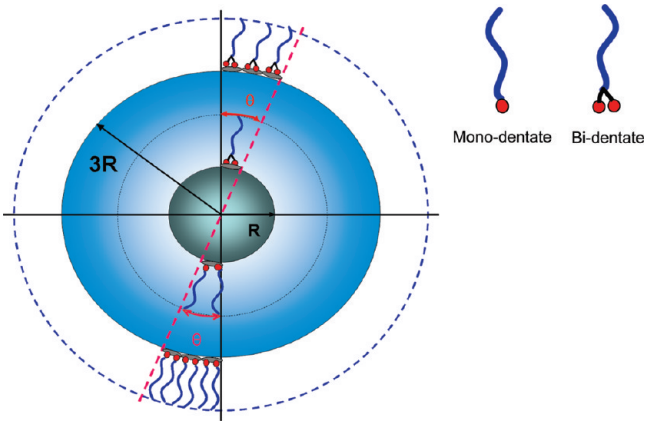

Figure 7. Schematic representation of the effects of packing versus coordination number on the NP stability: dithiol-PEG (top section) and monothiol-PEG (bottom section). The footprint is the area occupied by an anchoring group on the surface. For a similar angle θ, the higher curvature (for smaller NPs) produces more freedom for ligands to sample available space and less shielding of the surface. Thus, NP stability is dominated by the coordination number of the ligand. Conversely, lower curvature (for larger NPs) produces better packing of ligands and less space for ligand sampling; thus, higher density for HS-PEG-OCH_3 ligands is permitted on the larger nanoparticles.

larger sampling space for the ligand tail (compared to larger nanocrystals). This results in a "loosely" packed ligand layer on the smaller NPs and thus less shielding of the nanocrystal surface. In this regime, the affinity of the anchoring group of the ligand to the surface becomes the dominant factor in defining the NP resistance against cyanide digestion. That is why for 5 nm nanocrystals, TA-PEG-OCH_3-AuNPs exhibited a slower digestion rate than HS-PEG-OCH_3-AuNPs as shown in Figure 6A. Conversely, larger nanoparticles present a smaller surface curvature, which reduces the lateral space to be sampled by the hydrophilic PEG tails for the same footprint. This implies that the packing of the ligand tails is tighter on larger nanocrystals. Because HS-PEG-OCH_3 presents a smaller footprint (single thiol), the resulting AuNPs will have a higher overall ligand density. A higher density of packing would also favor a stronger interaction between the 6-carbon alkyl chains that then act as a hydrophobic barrier to protect the inorganic core from NaCN. Cyanide digestion is weaker for monothiol-capped nanoparticles in this case, as shown in Figure 6C for 15 nm AuNPs. The 10 nm NPs present an intermediate regime where the effects of the coordination number and ligand packing density are balanced. This produced similar digestion rates for both sets of samples. An ongoing topic of interest has been the effects of packing versus the geometrical extension of surface ligands; it has driven the development of dendritic ligands as well as the investigation of the effect of branching chemical structures.[12,32,37] The present study further complements those findings.

Conclusions

We have explored the effects of varying the coordination number on the affinity of molecular-scale ligands to the surface of Au nanoparticles. We carried out several stability experiments on AuNPs cap exchanged with either thiol-terminated PEG-OCH_3 or dithiolane-appended PEG-OCH_3 ligands. We found that ligands presenting a higher coordination number (dithiolane) exhibit much better stability to excess salt and against competition from DTT compared to their monodentate counterparts. However, stability to NaCN digestion showed that there are added benefits

of multidentate ligands to NP stability for the smaller nanoparticles, where a larger surface curvature could permit easier access of small molecules in the surrounding solution to the NP surface. Nonetheless, resistance to NaCN digestion indicated a more "nuanced" behavior. We found that in addition to the coordination number the packing density of the ligands could also play an important role in the dispersion stability. There is a clear balance between these two parameters, which is manifested in size- and coordination number-dependent digestion curves. For smaller NPs, a higher coordination is clearly beneficial, whereas a higher ligand density permitted by a lower curvature (characteristic of larger NPs) would make monodentate-capped nanoparticles more resistant to cyanide digestion. The benefits of using higher-coordination-number ligands for capping these metallic NPs are substantial in biology because media rich in excess ions are often used in biological assays. Resistance to DTT offered by TA-PEG ligands, for example, is a very important result because it indicates that there is an added benefit of strong ligand−NP interactions against competition from a whole array of small molecules in biological media.

Acknowledgment. We acknowledge NRL, Office of Naval Research (ONR), the Army Research Office, and the University of Massachusetts—Amherst for financial support. E.O. is supported by a fellowship from the Korea Research Foundation (D00089). We also thank Igor Medintz at NRL for assistance with some experimental details.

Supporting Information Available: Detailed information on the synthesis of HS-$(CH_2)_5$-PEG750-OCH_3 ligands, cap exchange of citrate-functionalized nanocrystals with TA-PEG750-OCH_3 and HS-PEG750-OCH_3 ligands, DTT and cyanide digestion tests, and an estimate of surface atoms on a given size of nanocrystals. This material is available free of charge via the Internet at http://pubs.acs.org.